Synthetic Aperture Method in Ultrasound Imaging

Ihor Trots, Andrzej Nowicki, Marcin Lewandowski and Yuriy Tasinkevych

Institute of Fundamental Technological Research
Poland

1. Introduction

Medical ultrasound imaging is a technique that has become much more prevalent than other medical imaging techniques since it is more accessible, less expensive, safe, simpler to use and produces images in the real time. However, images produced by an ultrasound imaging system, must be of sufficient quality to provide accurate clinical interpretation. The most commonly used image quality measures are spatial resolution and image contrast which can be determined in terms of beam characteristics of an imaging system: beam width and side-lobe level. In the design of an imaging system, the optimal set of system parameters is usually found as a trade-off between the lowest side-lobe peak and the narrowest beam of an imaging system.

In conventional ultrasound imaging system, when one transducer (in mechanical wobble) or linear array are used, the quality of images directly depends on the transducer acoustic field. Also in conventional ultrasound imaging the image is acquired sequentially one image line at a time that puts a strict limit on the frame rate that is important in real-time imaging system. Low frame rate means that moving structures (e.g. heart valves) are not easily imaged and diagnosis may be impaired. This limitation can be reduced by employing synthetic aperture (SA) imaging. The basic idea of the SA method is to combine information from emissions close to each other. The synthetic aperture method has previously not been used in medical imaging. This method is a contrast to the conventional beamforming, where only imaging along one line in receiving is used. This means that every image line is visualized as many times as the number of elements used. This will create an equal amount of low resolution images, which are summed up to create one high resolution image.

Problems with medical ultrasound include low imaging depth, and high resolution is achieved only in the region where the transducer is focused. Another problem is decreasing SNR with depth. The basic idea with synthetic aperture is to combine information from emissions close to each other. This is a contrast to the conventional beamforming, were only imaging along one line in receiving is used. This means that every image line is visualized as many times as the number of elements used. This will create an equal amount of low resolution images which are summed up to create one high resolution image.

One of the important processes in ultrasound imaging systems is beamforming. There are many different beamforming methods. In this work both the synthetic transmit aperture (STA) (Trots, et al. 2009) and the multi-element STA (Trots, et al. 2010) methods for medical ultrasound imaging system are discussed. In the case of the multi-element STA imaging

method a small number of elements is used to transmit a pulse and all array elements receive the echo signals. The main objective of this method is to increase system frame rate and the penetration depth, maintaining the resolution of images, so that smaller objects can be distinguished. Larger penetration depth can be obtained by increasing transmitted energy that allows increasing the SNR and in its turn to improve the ultrasound image contrast.

Ultrasound imaging systems usually use from 64 to 128 transmit/receive channels. In order to lower the cost of the system, the number of channels should be reduced.

2. Synthetic aperture method

2.1 Synthetic transmit aperture method

As an alternate to the conventional phased array imaging technique the STA method (Hongxia, 1997; Trahey & Nock, 1992) can be used. It provides the full dynamic focusing, both in transmit and receive modes, yielding the highest imaging quality.

In the STA method at each time one array element transmits a pulse and all elements receive the echo signals, see Fig. 1. where data are acquired simultaneously from all directions over a number of emissions, and the full image can be reconstructed from these data. The advantage of this approach is that a full dynamic focusing can be applied to the transmission and the receiving, giving the highest quality of image.
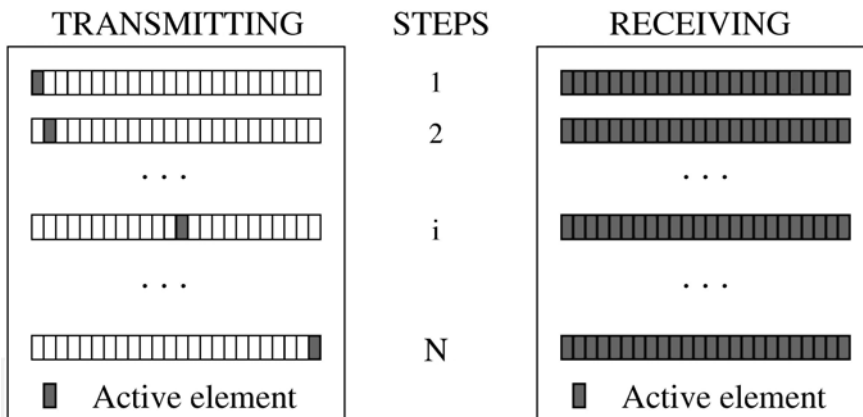

Fig. 1. Transmitting and receiving in STA method

In the STA method focusing is performed by finding the geometric distance from the transmitting element to the imaging point and back to the receiving element. The structure of the synthetic aperture and geometric relation between the transmit and receive element combination is shown in Fig. 2.

When a short pulse is transmitted by element m and the echo signal is received by element n, as shown in Fig. 2, a round-trip delay is

$$\tau_{m,n} = \tau_m + \tau_n ,\tag{1}$$

where (m, n) is a transmit and receive element combination, $0 \le m, n \le N–1$.
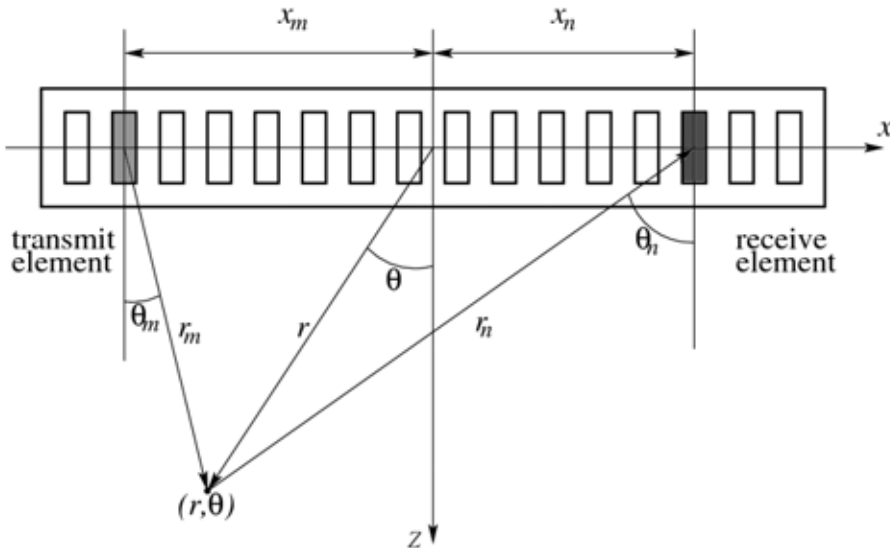
Fig. 2. Geometric relation between the transmit and receive element combination and the focal point

The delays for m'th element and n'th element are

$$\tau_m = \frac{1}{c}\left(r - \sqrt{x_m^2 + r^2 - 2x_m r \sin\theta}\right), \tau_n = \frac{1}{c}\left(r - \sqrt{x_n^2 + r^2 - 2x_n r \sin\theta}\right),\tag{2}$$

where x_m, x_n are the positions of the m'th and n'th elements, respectively and r is a distance between synthetic aperture centre and the point (r,θ). For an N-element array for each point in an image, the A-scan signal can be expressed as

$$A(r,\theta) = \sum_{m=0}^{N-1}\sum_{n=0}^{N-1} y_{m,n}\left(\frac{2r}{c} - \tau_{m,n}\right),\tag{3}$$

where $y_{m,n}(t)$ is the echo signal and $\tau_{m,n}$ is beamforming delay for the (m, n) receive and transmit element combination given in eq. (1). The first and second summations correspond to transmit and receive beamforming.

2.2 Multi-element synthetic transmit aperture

The multi-element STA imaging method represents the best solution in improving lateral resolution and penetration depth. It is known that the lateral resolution can be improved by increasing array length. Only a small number of elements are used to transmit a pulse but all array elements receive the echo signals. In practice, it is not very expensive to build a large transmit aperture, but it is very complex to form a large receive aperture. For a transmit pulse (from all transmit subaperture elements), the RF echoes for all receive elements are stored in memory. When all RF echo signals have been acquired, the total RF sum is formed by coherently adding them.

The multi-element STA method is proposed to increase the system frame rate and the speed of the image acquisition is determined by the number of transmissions M (Fig. 3). For an N-element aperture, M×N data recordings are needed for image reconstruction, where M<<N.
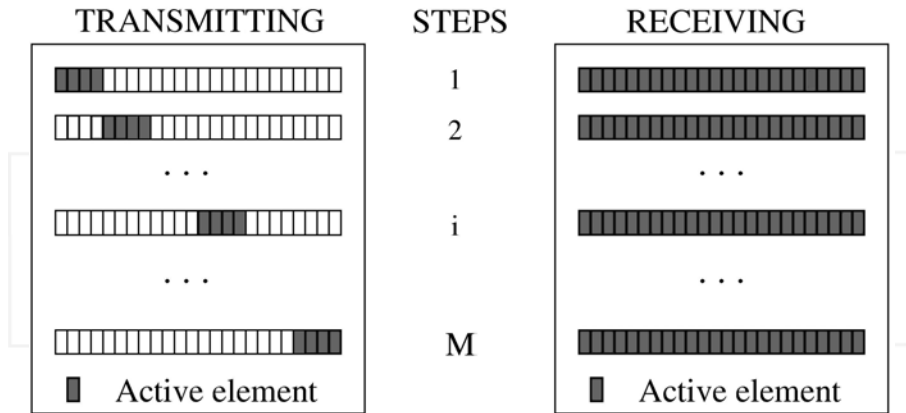

Fig. 3. Transmitting and receiving in multi-element STA method

The geometrical locations of the transmit elements in a multi-element array system impacts the radiation pattern of that system, which in its turn impacts lateral resolution of the image, whereas the number of active transmit elements directly influences the transmitted energy and the SNR. These parameters define the ultrasound image quality. Therefore, the optimization of a multi-element STA imaging system can be formulated as an optimization problem of the location and the number of the transmit elements. The main optimization criterion in the multi-element STA method is the minimal width of the main-lobe combined with the minimum side-lobe level. This optimization leads to increasing image penetration depth and high lateral resolution.

For an N-element array, the transmit aperture is split into Ns subapertures with $K_t=N/Ns$ elements each (Hongxia, 1997). Each subaperture transmits a prefocused beam with focus point near the middle of the region of interest. Echo signals reflected from objects are received at a full or dynamically varying receive aperture with dynamic focusing, and stored in memory. Then data recordings must be focused synthetically with dynamic transmit focusing.

Fig. 4 shows the geometry of the transmission and the reception for the STA system, where $(r; \theta)$ is the point of focus.

The transmit delay has two parts. The first part is the delay to focus all the elements in the subaperture towards the focal point. The second part is the delay to focus all subapertures dynamically. The first part of the delay for the m'th element in the subaperture is

$$\tau_m = \frac{r_s - r_{tm}}{c} \tag{4}$$

$$r_{tm} = \sqrt{\left[\left(-\frac{K_t-1}{2}+m\right)d\right]^2 + r_s^2 - 2\left(-\frac{K_t-1}{2}+m\right)dr_s \sin\alpha}$$
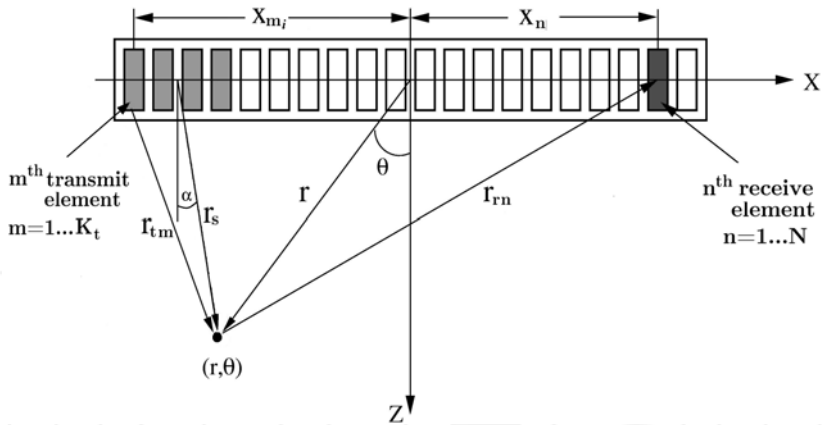
Fig. 4. Geometric relation between the transmit and receive element combination and the focal point

and

$$\alpha = \cos^{-1}\left(\frac{r\cos\theta}{r_s}\right).$$

The second part of the delay for the i'th subaperture is

$$\tau_i = \frac{r - r_s}{c} = \frac{1}{c}\left(r - \sqrt{(r\cos\theta)^2 + (xm_i - r\sin\theta)^2}\right) \tag{5}$$

$$= \frac{1}{c}\left(r - \sqrt{\left[K_t\left(-\frac{N_s - 1}{2} + i\right)d\right]^2 + r^2 - 2K_t\left(-\frac{N_s - 1}{2} + i\right)dr\sin\theta}\right)$$

The receive delay τ_n for the STA can be obtained in a similar way as for the phased array

$$\tau_n = \frac{(r - r_{rn})}{c}. \tag{6}$$

Thus, the total delay is $\tau_m + \tau_i + \tau_n$.

For each image point $(r;\theta)$, the A-scan signal is

$$A_{STA}(t) = \sum_{n=0}^{N-1}\sum_{i=0}^{N_s-1}\sum_{m=0}^{K_t-1} s_{K_i i+m,n}(t - \tau_n - \tau_i - \tau_m), \tag{7}$$

where $s_{m,n}(t)$ is the echo signal. The first summation corresponds to the receive beamforming, while the second and the third summations correspond to the transmit synthetic aperture beamforming.

3. Element directivity diagram influence

In the described above beamforming methods for each point in the resulting image every combination of transmit-receive pairs contributes according to the round-trip propagation time only. The angular dependence is not taken into account in the applied point-like source model. But when the width of the array element is comparable to the wavelength corresponding to the nominal frequency of the emitted signal, the point-like source model becomes inaccurate. The element directivity influences the partial contribution to the resulting signal $A(r, \theta)$ in eq. (3) depending on the mutual position of the imaging point and transmit- receive pair, determined by the angles θ_m, θ_n (see Fig. 2). Here, a modified STA imaging algorithm, which accounts for the element directivity function and its influence on $A(r, \theta)$, is developed (Tasinkevych, et al. 2010).
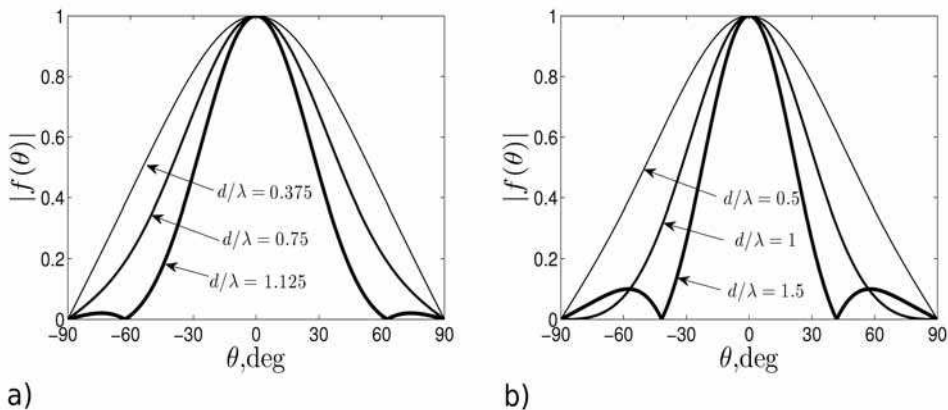

Fig. 5. Directivity function for different values of d/λ

The underlying idea can be illustrated on the following example, shown in Fig. 6. Here, it is assumed, that the same element transmits and receives signal. Two scatterers located at the points with polar coordinates (r_i, θ_i), $i=1,2$ such that $r_{1m}=r_{2m}$ would contribute to the corresponding echo signal $y_{m,m}(t)$ simultaneously, since the round-trip propagation time $2r_{im}/c$, $i=1,2$ is the same (the corresponding numerical example is shown in Fig. 3 in the next section). Apparently, the contribution from the scatterer at the point (r_1, θ_1) would be dominant, since the observation angle θ_{1m} coincides with the direction of maximum radiation for the m-th element, whereas its transmit-receive efficiency at the angle θ_{2m} is much smaller for the case of the scatterer at the point (r_2, θ_2). Thereby, evaluating the value of $A(r_2, \theta_2)$ from eq. (3), the partial contribution of the echo $y_{m,m}(t)$, in addition to the correct signal from the obstacle located at (r_2, θ_2) (being small due to the large observation angle θ_{2m}), would also introduce the erroneous signal from the scatterer located at (r_1, θ_1). The latter signal is larger due to the small observation angle θ_{1m}. The larger observation angles appear in the imaging region close to the array aperture. Therefore, the most appreciable deviation from the point-like source model of the array element will occur there. A solution to the problem, which accounts for the observation angle in accordance with the array element directivity function, is proposed. Assume, that the dependence of the

transmit-receive efficiency of a single array element versus the observation angle is known and is denoted by $f(\theta_m)$, where θ_m is measured from the line parallel to z-axis and passing through the m-th element center. Thus, in order to suppress the erroneous influence from the scatterer located at (r_1, θ_1) on the value of the resulting signal $A(r_2, \theta_2)$, the partial contribution of the echo $y_{m,m}(t)$ is weighted by the corresponding value of $f(\theta_{2m})$. This corresponds to the superposed signal correction in accordance with respective contributions of individual scatterers located at the points (r_1, θ_1) and (r_2, θ_2) (Fig. 6).
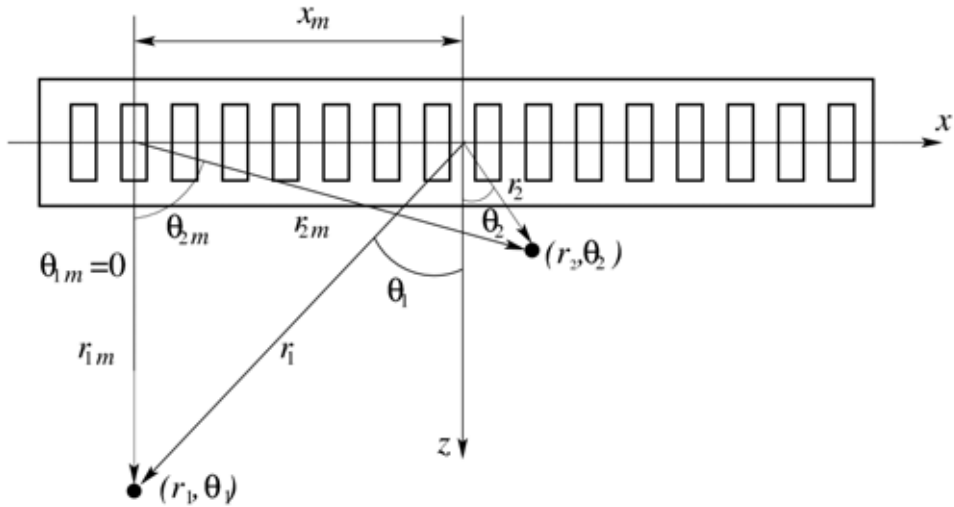

Fig. 6. Influence of the scatterer located at the point (r_1, θ_1) on the value of resulting signal $A(r_2, \theta_2)$ for imaging point (r_2, θ_2)

The above considerations lead to the following modification of the synthetic focusing imaging algorithm

$$A(r,\theta) = \sum_{m=1}^{N}\sum_{n=1}^{N} f(\theta_m)f(\theta_n)y_{m,n}\left(\frac{2r}{c} - \tau_{m,n}\right) , \qquad (8)$$

where $\theta_i(r, \theta)$, $i=m,n$ are the corresponding observation angles for the transmit-receive pair. The modification of the STA thus is expressed by weighted summation of properly delayed RF signals (as in the case of conventional STA). The corresponding weights $f(\theta_m)$, $f(\theta_n)$ in the transmit and receive modes are calculated by means of the single element directivity function. Note, that the angles depend on the spatial location of the imaging point (r, θ). The directivity function $f(\theta)$ can be calculated in the far-field approximation for a single element of the array transducer in analogous manner as in (Selfridge, et al. 1980) (see example in Fig. 5)

$$f(\theta) = \frac{\sin(\pi d / \lambda \sin \theta)}{\pi d / \lambda \sin \theta}\cos \theta \qquad (9)$$

where d is the element width, and λ is the wavelength. Some examples of the directivity function evaluated for different values of the ratio d/λ are shown in Fig. 5. Note, in Fig. 5b the values of d/λ correspond to the case when the element width d=0.75*pitch, and the pitch is 0.5, 1, and 1.5 of the lambda, respectively. The above result applies to a narrow strip transducer with a time harmonic uniform pressure distribution along its width. It is obtained by means of the Rayleigh-Sommerfeld formula in the far-field region. The result is in a good agreement with experimental studies as shown by the authors in the cited work. For simplicity, eq. (9) is applied in the numerical results presented in the next section. It should be noted, that we use the angular response $f(\theta)$ in eq. (8) evaluated from eq. (9) for some fixed value of λ, which corresponds to the nominal frequency of the transmitted signal. The far-field approximation is admissible for the case of synthetic focusing algorithm discussed here. For the typical examples considered in the next section, the ratio d/λ =1.125 is assumed, and the coresponding element directivity function is depicted in Fig. 5b. The far-field limit $r_{min} \approx 2d^2/\lambda$ (Michishita, et al. 2000) is 2.5λ. This requirement is met in the considered numerical experiments.

4. Computer simulation

Simulation is a fundamental way of testing methods. This is done to confirm or reject a hypothesis in a controlled environment. Since it is possible to control all parameters in a simulation, one can set up a simple model and then gradually transform it into something more similar to reality. When this is done one can continue with measurements and confirm or reject the simulations for a real setup, in vivo or on a phantom. All simulations in this work are carried out with a powerful software, *Field II* (Jensen, 1999). The program is developed especially for investigating ultrasound fields, and gives the possibility to simulate and calculate ultrasound fields and defining one's own transducer. The accuracy is very high since *Field II* is based on numerical analysis. *Field II* runs under Matlab which makes it even more versatile and useful. This is the reason why *Field II* is used worldwide.

The numerical results presented in Fig. 7 and Fig. 8 were performed for a 48-element linear transducer array excited by one sine cycle burst pulse at a nominal frequency of 5 MHz. The element pitch is 1.5λ and the inter-element spacing is 0.25 of the pitch, where λ corresponds to the nominal frequency of the burst pulse. The STA algorithm is employed. The transmit and receive elements combinations give a total of 48×48 possible RF A-lines. All these A-lines echo signals are sampled independently at a frequency of 50 MHz and stored in RAM.

In Fig. 7 a numerical example explaining the discussion of the previous section is shown. Two point scatteres are placed at different depths: one in the immediate vicinity of the transducer element and another is located deeper, as depicted in Fig. 6.

The blurring of the scatterer placed near the aperture is significantly diminished in the case of introducing the directional diagram of element in synthetic focusing algorithm as compared to the algorithm without this correction, being in agreement with the above consideration of section 3.

In Fig. 8 the results of simulation of a wire phantom are shown. Thin wires are spaced equidistantly with raster of 6λ in the lateral and axial directions. Fig. 8a (left) corresponds to the algorithm eq. (8) with the angular directivity function calculated according to (9), whereas in Fig. 8a (right) the results corresponding to the algorithm eq. (3) are shown for comparison.
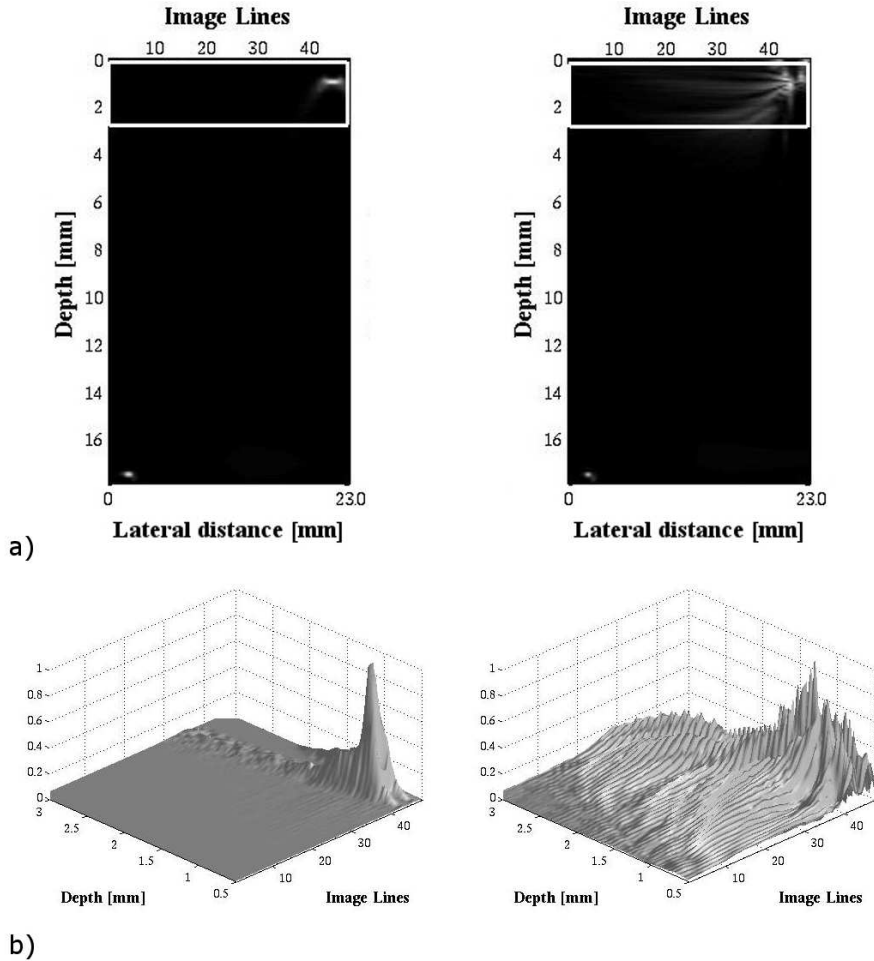
Fig. 7. Simulation of 2 point scatterers for 48-element linear array: a) left subplot – including directional diagram of element, right subplot – not including directional diagram of element; b) detailed view of the selected part of the images in (a), respectively. The magnitude of the scattered field in a linear scale is shown

The simulation results have shown distinguishable improvement of the imaging quality of the scatterers situated in the region near the transducer aperture. The artefacts in the form of hazy blurring, observable in the conventional STA algorithm are substantially suppressed in the case of the modified one. Besides, the imaging depth is also increased, which is the valuable advantage of the developed method.
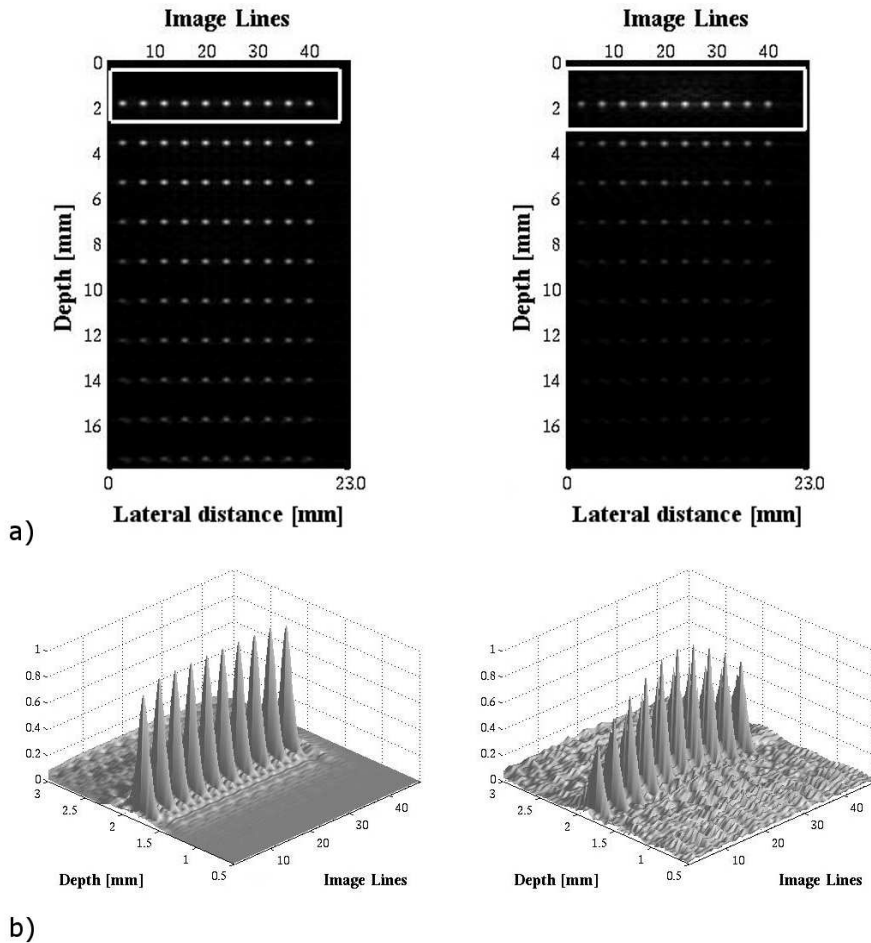
Fig. 8. Thin wire phantom simulation using a) left subplot - including directional diagram of element, right subplot - not including directional diagram of element; b) detailed view of the selected part of the phantom including and not including directional diagram of element, respectively. The magnitude of the scattered field in a linear scale is shown

In the next part of simulation the parameters used in the simulations are set to be similar to those of transducer used in the measurements. The medium in the simulations is homogeneous and its only variable parameter is the speed of sound. In the simulations no attenuation is considered. Even so, echoes far from the transducer become weaker and have lower amplitude because the energy is spread out. These simplifications do not affect the method in principle and in measurements these simplifications have been taken into account.

In Fig. 9 the 2D ultrasound images of phantom, obtained by computer simulation for the case of 32-element linear transducer array with 0.48 mm inter-element spacing and one-cycle burst pulse at nominal frequency 5 MHz, are shown. In the case of multi-element STA method every subaperture consists of the two elements and transmits an unfocused ultrasound wave. The phantom medium attenuation is 0.5 dB/[MHz×cm] and consists of the collections of point targets spaced 4 pitches apart laterally, and the collections are spaced axially 5 mm apart from each other.
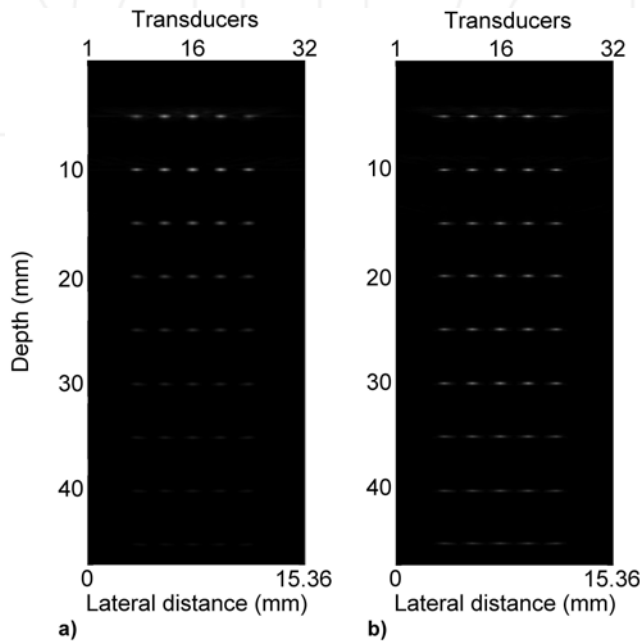
Fig. 9. The 2D ultrasound images of phantom with point targets for the STA method (a) and the multi-element STA (b)

It can be easily seen, that penetration depth increases in the case of the multi-element STA. For the objective comparison of the resolution the axial cross sections of the centre line and lateral cross sections in the depths 10 mm and 20 mm are shown in Fig. 10.

Fig. 10 shows that transmitted energy grows in the multi-element STA method and the penetration depth increases while lateral resolution is comparable in both cases.

The multi-element STA imaging method represents the best solution in improving penetration depth and maintaining lateral resolution.
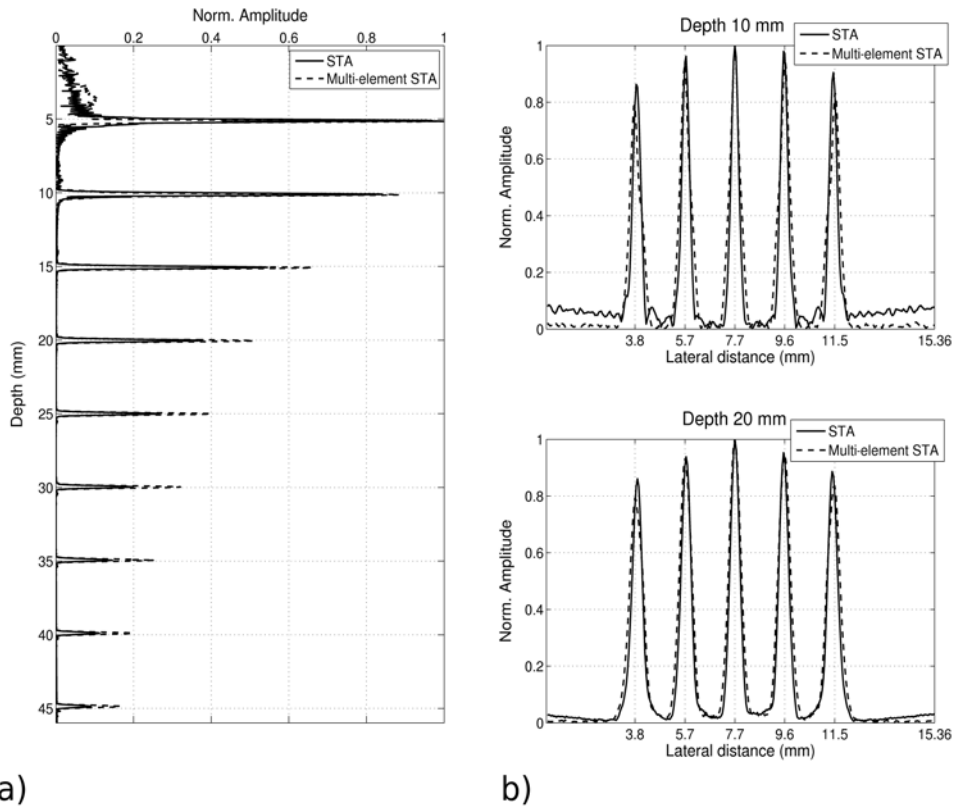
Fig. 10. Comparison of the cross sections between STA method and multi-element STA method: a) axial cross section of the centre line; b) lateral cross section in depth 10 mm (top) and depth 20 mm (bottom)

5. Ultrasound imaging system

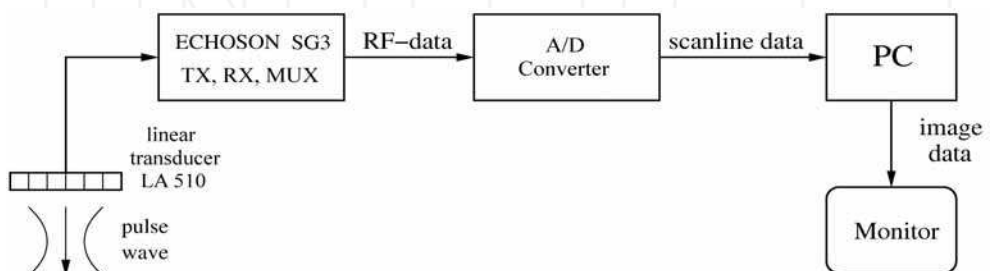Synthetic aperture evaluation was performed using a simplified ultrasound imaging system which is shown in Fig. 11.

Fig. 11. Block diagram of the ultrasound imaging system

Linear transducer LA510 produced by Echoson (Echoson, Pulawy, Poland) transmits pulsed ultrasound waves, and receives reflected echo signals. Echoson SG3 transmitting/receiving system enables full control of selected 32 consecutive channels/transducers of a linear array transducer. Parameters of transmission and reception are programmable from a PC using a serial port (RS-232). Using the SG3 one can switch on arbitrary transmit and receive channels in the selected 32 channels aperture. The second block, A/D converter extracts the RF data, acquires it and sends to the PC. Next, the collected digital data were processed offline and displayed on the monitor. All post processing and display is done on the computer using Matlab™ software. The processing creates 2D ultrasound imaging focused in every point of image.

The system allows performing simulated multichannel acquisition for synthetic aperture imaging. Using a single channel digitizer and switching receiving transducers the system is capable of gathering the RF data for up to 32 lines. Repeating this procedure for each transmitted element of the N-element transducer the N×N data recordings are obtained with the STA method or the M×N data with the multi-element STA method, where M is subaperture number, needed for image reconstruction. These data are the input to the synthetic aperture algorithm.

Synthetic aperture image reconstruction requires considerable amount of data storage and processing power. The amount of raw RF data needed in the STA imaging for reconstruction of a single image is proportional to $D_{RF} * N^2$, and the number of delay-and-sum operations is $D_{RF} * N^3$, where D_{RF} is the number of samples in a single RF line. For 32 elements linear array with 15 cm penetration (D_{RF}=8000 at 40 MHz sampling frequency) storage requirements $\approx$ 8.2*10⁶ samples, delay-and-sum operations $\approx$ 262*10⁶ are obtained.

The multi-element STA method imaging allows to reduce the amount of raw RF data needed for reconstruction of a single image and is equal to $D_{RF} * M * N$ and the number of delay-and-sum operations is $D_{RF} * M * N^2$. For 32 elements linear array and 2 elements in subaperture (M=16) with 15 cm penetration storage requirements $\approx$ 4.1*10⁶ samples, delay-and-sum operations $\approx$ 131*10⁶ are obtained. It is two times less than in the case of classical STA method.

6. Experimental results and discussion

The 32-element linear transducer array with 0.48 mm inter-element spacing and a burst pulse with time duration of 100 ns (a half-cycle at nominal frequency 5 MHz) were used in experiments. The inter-element spacing is about 1.5λ. All elements are used for both the transmitting and receiving. An element in the transducer transmitting aperture was used to generate a spherical wave covering the full image region. The received echo signals were sampled independently at 50 MHz and then stored.

Firstly, the experiments were performed using the standard STA method in which one array element transmits a pulse and all elements receive the echo signals. In this experiments the wire phantom was used, that consists of 24 wires 0.1 mm in diameter, positioned axially every 2 mm at an angle of 75 degrees. This phantom allows to examine the axial and lateral resolution at various depths in the ultrasound image, as well as the focal and dead zone registration. Since the phantom was immersed in water, where there is almost no attenuation, high amplitude echo signals from the wires were obtained.

Three of 1024 (32x32) received RF echo signals, which were digitized and stored in the PC, are shown in Fig. 12.
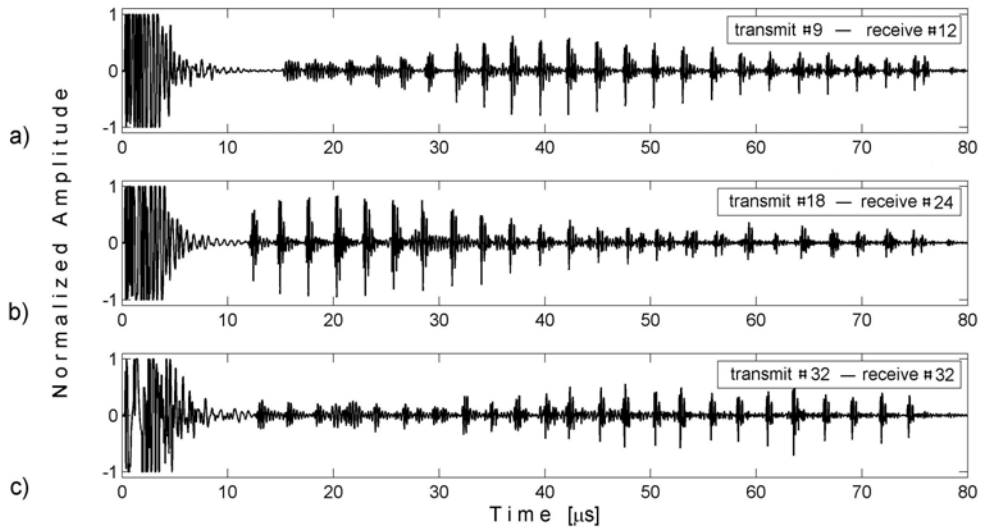
Fig. 12. The recorded by PC RF echo signals: a) element #9 is transmitting – element #12 is receiving, b) #18 transmitting – #24 receiving, c) #32 transmitting – #32 receiving

All these RF echo signals are different and echo time position and signal amplitude in every case depend on sound field and geometrical position of transmitted and received transducers. After all emissions the full set of the RF A-lines echo signals, needed to reconstruct one 2D B-mode ultrasound image, is obtained. For this aim the synthetic aperture algorithm calculates the time delays and weights resulting from the directivity function for every combination of transmit-receive pairs and current imaging points and from the RF-lines computes the final image.

As was mentioned above, a single element in the transducer aperture is used for transmitting a spherical wave covering the full image region. The received signals for all or part of the elements in the aperture are sampled for each transmission. This data can be used for producing low resolution images (Fig. 13a – 13c), which is only focused in the receive due to the unfocused transmission. Focusing is performed by compensating the geometric distance from the transmitting element to the imaging point and back to the receiving element and can be obtained from eq. (3). These low resolution images need to be added coherently to form the final high resolution image (Fig. 13d).

Fig. 13 presents the standard STA imaging method, where at each time one array element transmits and all elements receive. This method represents a good solution when small N-elements array transducers are used. In present ultrasound diagnostic the 128- or 192-elements array transducers are used and application of such STA method restricts the image acquisition considerably. For this purpose the multi-element STA method is proposed where two elements in subaperture transmit a flat ultrasound wave and are shifted by one subaperture that allows to increase the speed of the image acquisition.

To compare the multi-element STA method and standard STA method the tissue mimicking phantom, model 525 Danish Phantom Design, with attenuation of background material 0.5 dB/[MHz×cm], was used in experiments.

In Fig. 14 two of 512 (16x32) received RF echo signals, which were digitized and stored in the PC, are shown.
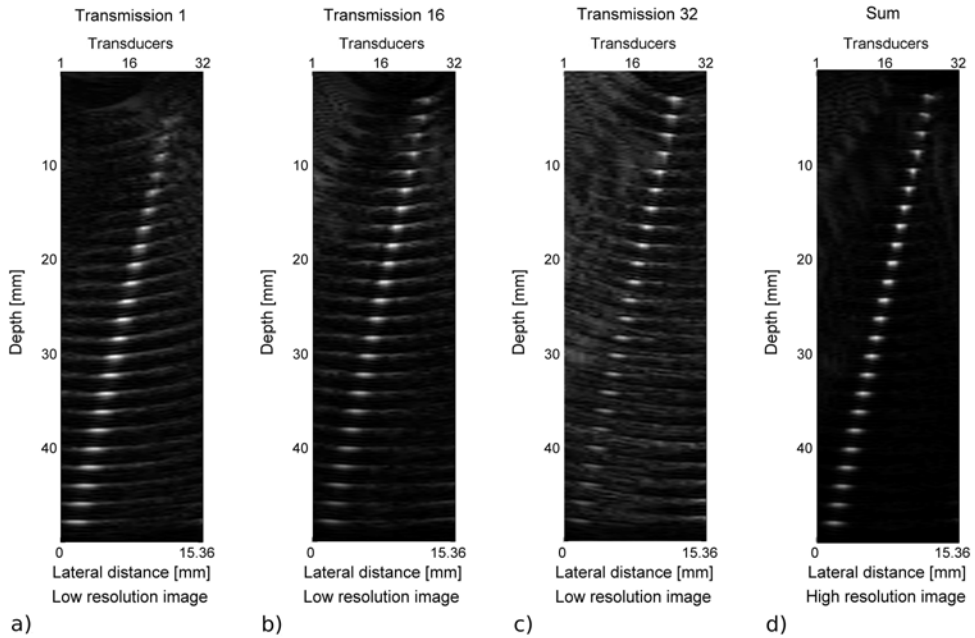
Fig. 13. Low resolution images combined to produce a high resolution image. One element transmit at the time, while all are used to receive. The images are then added into one high resolution image
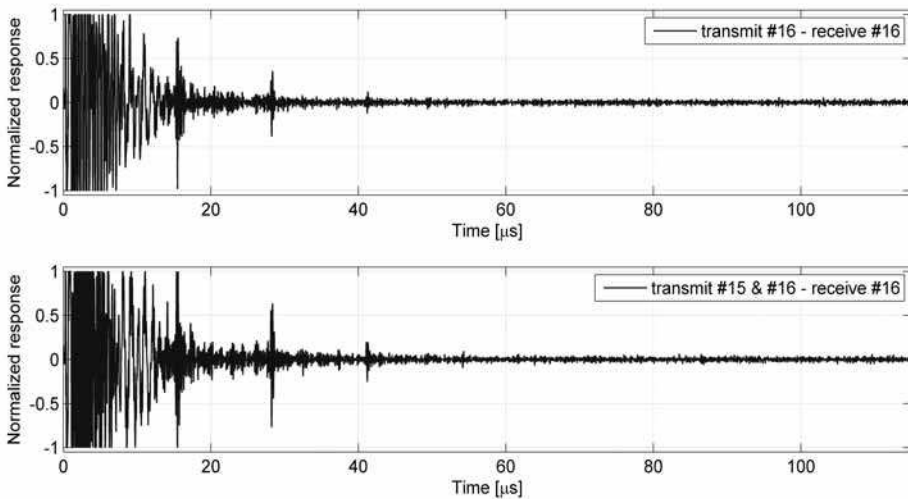

Fig. 14. The recorded echo signals: a) the STA method - element #16 is transmitting – element #16 is receiving, b) the multi-element STA method - elements #15 and #16 transmitting – #16 receiving

It can be easily seen, that the amplitude of the echo signals in the multi-element STA method is about two times higher.

The comparison of the 2D ultrasound images of the tissue phantom, obtained with the standard STA method and multi-element STA method, are shown in Fig. 15.
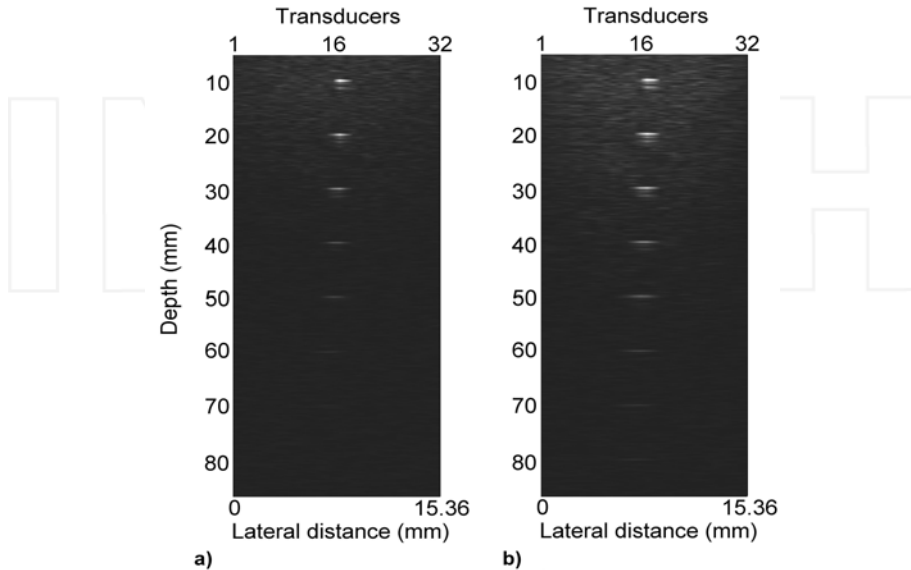

Fig. 15. 2D ultrasound images of tissue mimicking phantom: a) using STA method; b) using multi-element STA method

The obtained 2D ultrasound images clearly demonstrate the advantage of the multi-element STA method. With the elongation of the transmit aperture the acoustical power increases yielding a higher SNR, that leads to an increase in the penetration depth while maintaining both axial and lateral resolution. The last resolution depends on transducer acoustic field and is discussed in (Nowicki et al., 2007).

In order to compare quantitatively the SNR gain the central RF-lines of the 2D ultrasound images shown in Fig. 15 are in Fig. 16 and the SNR is calculated.

Fig. 16 shows that increasing transmitted aperture by one element improves the SNR by about 5 dB that in one's turn leads to improvement of the penetration depth and the contrast of the image.

The next part of the experiments was to compare the 2D B-mode ultrasound images obtained using the STA method and the standard linear array scanning method that is applied in commercial ultrasound scanner Antares (Siemens, Mountain View, CA, USA). In this experiments the wire phantom was used. In the STA method the linear transducer array (LA510) with 0.48 mm inter-element spacing and a burst cycle pulse at nominal frequency 5 MHz, while in the ultrasound scanner Antares the linear transducer array with 0.3 mm pitch (VF13-5) and a burst cycle pulse at nominal frequency 10 MHz, were used.

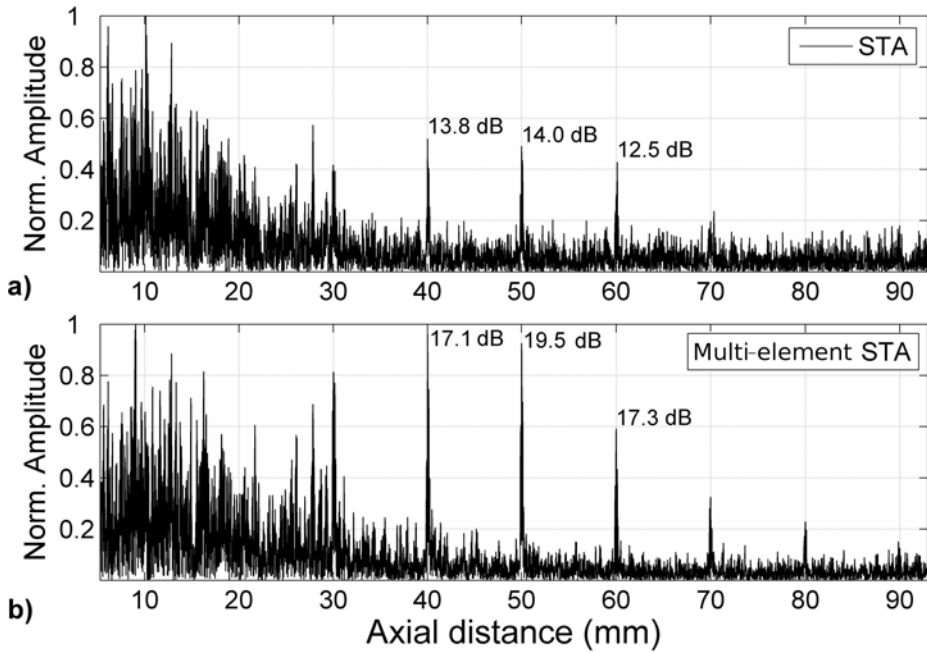Focus principle in ultrasound scanner Antares is shown in Fig. 17.

Fig. 16. The RF-lines of the tissue mimicking phantom: a) using STA method; b) using multi-element STA method
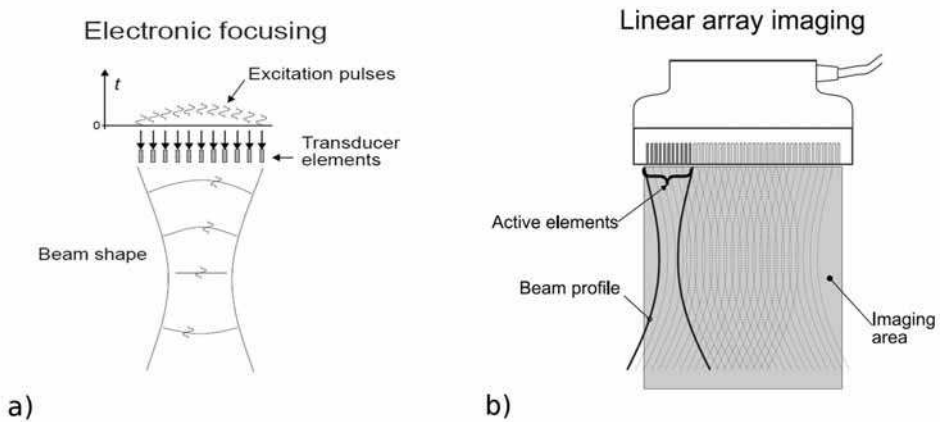

Fig. 17. a) electronic focusing principle; b) linear array transducer for obtaining a rectangular cross-section image

The comparison of the reconstructed wire phantom images, obtained using the STA method and standard linear array scanning with commercial ultrasound scanner Antares, is shown in Fig. 18. The maximum quantity of focal points, which were equal to 1 and 8, were chosen in the ultrasound scanner; they are marked by little triangles at the bar side.
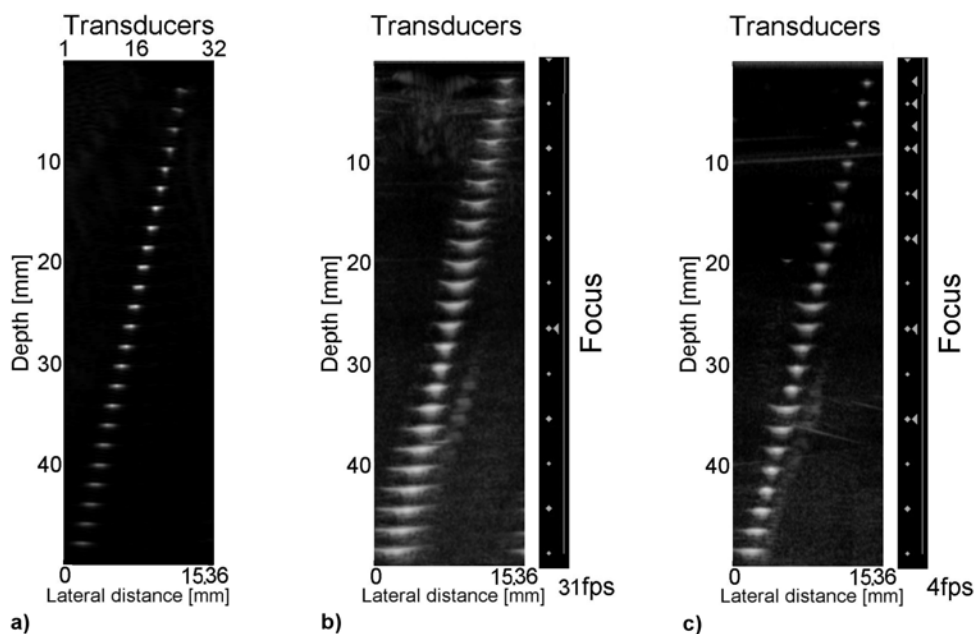
Fig. 18. The 2D ultrasound images of the wire phantom: a) using STA method; b) ANTARES ultrasound scanner with one focal point; c) ANTARES ultrasound scanner with 8 focal points

In Fig. 18 it can be easily seen, that axial and lateral resolutions at the top and at the bottom parts of the image are different and depend on the focal point quantity in these regions. It needs to be noted, that frame rate in the case 8 focal points dramatically decreases down to 4 fps (in the case of one focal point it is equal to 31 fps). Such frame rate is definitely insufficient to examine in a standard way the dynamically moving organs, such as heart, where high frame rate even up to 50 fps is required.

The obtained 2D images show that the STA method allows obtaining good resolution in the whole explored region maintaining the high frame rate. Also, the results show the effectiveness of the STA method and its resistance to the refraction, attenuation, and reflection of ultrasound waves.

7. Conclusion

The STA method, being a variety of the synthetic aperture approach, is discussed. Its development and investigation is presented. The main advantage of the STA method is the increase of the system frame rate and thus substantial improvement of the image quality. Numerous examples of how the medical SA ultrasound imaging can be acquired and processed are shown. The conventional STA method and multi-element STA imaging algorithm are compared. In the latter case, more than one elements are used in transmit mode but all array elements operate in receive mode. It is shown, that even for two element transmit aperture the SNR can be improved by about 5 dB maintaining the same imaging

resolution as compared to the conventional STA. This, in its turn, allows to improve the penetration depth and makes the ultrasound image more contrast.

Also, the modified STA algorithm is presented. This algorithm is based on the array element angular directivity function implementation into the conventional STA method and corresponding correction of the back-scattered RF signals of different transmit-receive pairs. It is shown that the far-field radiation pattern of a narrow strip transducer, calculated for the case of a time harmonic uniform pressure distribution over its width, can serve as a good approximation for the above directivity function. The results of numerical calculations using simulated data, as well as experimentally obtained ones for different phantoms, have shown distinguishable improvement of the imaging quality of the scatterers situated in the region near the transducer aperture, the hazy blurring artefacts, observable in the case of conventional STA algorithm, are substantially suppressed.

Finally, the comparison of the ultrasound images reconstructed, using the STA method and by commercial ultrasound scanner Antares, is shown. The images reconstructed by the STA system give the same image resolution as that from the conventional ultrasound system with an increased frame rate. The STA system offers higher image resolution than conventional system if the frame rate is the same in both cases. The synthetic transmit aperture method can be applied in a standard ultrasound scanner. Introduction of the STA method in medical ultrasound would increase the efficiency and quality of the ultrasound diagnostic.

8. Acknowledgements

9. References

Jensen, J.A. Linear description of ultrasound imaging systems. (1999). *Notes for the International Summer School on Advanced Ultrasound Imaging,* Technical University of Denmark, June 10, 1999.

Hongxia, Y. (1997). *Synthetic aperture methods for medical ultrasonic imaging*. Thesis.

Michishita, K.; Sakagami,K,; Morimotgo, M.; Svensson, U.P. (2000). Sound radiation from an unbaffled elastic plate strip of infinite length. *Applied Acoustics,* Vol. 61, No. 1, pp. 45-63, S0003-682X(99)00067-5

Nowicki, A.; Klimonda, Z.; Lewandowski, M.; Litniewski, J.; Lewin, P.A.; Trots, I. (2007). Direct and post-compressed sound fields for different coded excitation, *Acoustical Imaging,* Vol. 28, No. 5, pp. 399–407, ISBN 978-1-4020-5720-5

Selfridge, A.R.; Kino, G.S.; Khuri-Yakub, B.T. (1980). A theory for the radiation pattern of a narrow-strip acoustic transducer. *Appl. Phys.Lett.,* Vol. 37, No. 1, pp. 35-36, ISSN 0003-6951

Tasinkevych, Y.; Nowicki, A.; Trots, I. (2010) Element directivity influence in the synthetic focusing algorithm for ultrasound imaging, *Proceedings of the 57th Open Seminar on Acoustics OSA 2010*, pp. 197-200, ISBN 978-83-931744-0-9, September 2010, Gliwice, Poland

Trahey, G.E.; Nock, L.F. (1992). Synthetic receive aperture imaging with phase correction for motion and for tissue ihomogeneities — part I: Basic principles. *IEEE Trans. Ultrason. Ferroelec. Freq. Contr.*, Vol. 39, No. 4, pp. 489–495, ISSN 0885-3010

Trots, I.; Nowicki, A.; Lewandowski, M. (2009). Synthetic transmit aperture in ultrasound imaging, *Archives of Acoustics*, Vol. 43, No. 4, pp. 685-695, ISSN 0137-5075

Trots, I.; Nowicki, A.; Lewandowski, M.; Tasinkevych, Y. (2010). Multielement synthetic transmit aperture in medical ultrasound imaging, *Proceedings of the 57th Open Seminar on Acoustics OSA 2010*, pp. 205-208, ISBN 978-83-931744-0-9, September 2010, Gliwice, Poland

Trots I., Nowicki A., Lewandowski M., Tasinkevych Y. (2010). Multi-element synthetic transmit aperture in medical ultrasound imaging, *Archives of Acoustics*, Vol. 35, No. 4, pp. 687 – 699, ISSN 0137-5075

Ultrasound Imaging

Edited by Mr Masayuki Tanabe

In this book, we present a dozen state of the art developments for ultrasound imaging, for example, hardware implementation, transducer, beamforming, signal processing, measurement of elasticity and diagnosis. The editors would like to thank all the chapter authors, who focused on the publication of this book.

How to reference

In order to correctly reference this scholarly work, feel free to copy and paste the following:

Ihor Trots, Andrzej Nowicki, Marcin Lewandowski and Yuriy Tasinkevych (2011). Synthetic Aperture Method in Ultrasound Imaging, Ultrasound Imaging, Mr Masayuki Tanabe (Ed.), ISBN: 978-953-307-239-5, InTech, Available from: http://www.intechopen.com/books/ultrasound-imaging/synthetic-aperture-method-in-ultrasound-imaging

INTECH
open science | open minds